Effect of impurities on the mechanical and electronic properties of Au, Ag, and Cu monatomic chain nanowires

D. Çakır* and O. Gülseren†

Department of Physics, Bilkent University, 06800 Ankara, Turkey

(Received 11 August 2010; revised manuscript received 11 August 2011; published 30 August 2011)

In this study, we have investigated the interaction of various different atomic and molecular species (H, C, O, H_2, and O_2) with the monatomic chains of Au, Ag, and Cu via total-energy calculations using the plane-wave pseudopotential method based on density functional theory. The stability, energetics, mechanical, and electronic properties of the clean and contaminated Au, Ag, and Cu nanowires have been presented. We have observed that the interaction of H, C, or O atoms with the monatomic chains are much stronger than the one of H_2 or O_2 molecules. The atomic impurities can easily be incorporated into these nanowires; they form stable and strong bonds with these one-dimensional structures when they are inserted in or placed close to the nanowires. Moreover, the metal-atomic impurity bond is much stronger than the metal-metal bond. Upon elongation, the nanowires contaminated with atomic impurities usually break from the remote metal-metal bond. We have observed both metallic and semiconducting contaminated nanowires depending on the type of impurity, whereas all clean monatomic chains of Au, Cu, and Ag exhibit metallic behavior. Our findings indicate that the stability and the electronic properties of these monatomic chains can be tuned by using appropriate molecular or atomic additives.

DOI: 10.1103/PhysRevB.84.085450 PACS number(s): 61.46.Km, 62.23.Hj, 73.22.−f, 73.20.Hb

I. INTRODUCTION

The fabrication of the stable gold monatomic chains suspended between two gold electrodes is one of the breakthroughs in nanoscience and technology, since the miniaturization of the electronic components is one of the significant cornerstones in the development and improvement of new devices in nanoelectronics. Nanowires show unusual mechanical, chemical, and electronic properties such as quantized conductance and much stiffer bonds compared to the ones in the bulk.[1,2] First, Ohnishi *et al.*[3] have visualized the monatomic chains by using transmission electron microscopy (TEM). At the same time, Yanson *et al.*[4] have produced the monatomic chain and they have measured its conductance. However, unusually long interatomic lengths have been measured, namely 3.5–4 Å, which is very large compared to those of bulk and dimer gold, in the bond-length measurements of these monatomic chains. Theoretical calculations on clean Au monatomic chains have revealed that it breaks before reaching such long interatomic distances.[5–11] Several explanations have been proposed in order to solve this puzzling experimental observation of long interatomic distances. For example, Sanchez-Portal and co-workers[12,13] have proposed a zigzag structure, where every second atom is fixed at its position, while the other atom rotates around the nanowire axis for a chain with an odd number of atoms. It has been argued that this rotation has been missed in TEM experiments. However, Koizuma *et al.*[14] have not found any evidence of spinning of gold atoms of these chain nanowires.

Another explanation is the presence of impurity atoms, such as C, H, or O, in chain nanowire structure.[15–27] These light impurity atoms cannot be imaged by TEM. Later, Au monatomic chains synthesized[28] under cryogenic vacuum at 4.7 K have retained interatomic distance as 2.5 ± 0.2 Å, which is consistent with the theoretical calculations. Furthermore, in order to explain the observed long interatomic distances, the electrical charging of the nanowire is also considered because of the fact that the excess charge might stabilize the longer bond lengths.[29]

Moreover, it has been shown that the tendency of evolving into monatomic chains of 5*d* metals is higher than that of 4*d* and 3*d* metals such as Ag and Cu.[30,31] As suggested by Smit *et al.*, the physical origin of this inclination of 5*d* elements might be related to *s*-*d* completion caused by relativistic effects.[32] The formation of suspended linear monatomic chains consequent to stretching of gold nanowires along the [110] crystal direction is studied by using density functional theory and tight-binding molecular dynamics (TBMD) calculations and it has been found that formation of single atomic chains can be possible only when the crystal symmetry is broken in the early elongation stages.[33] Note that thermal fluctuations or pulling of the wire along slightly off-axis can induce this crystallographic asymmetry. Furthermore, single chain Au nanowires are formed from Au wire under tensile deformation after several structural transformations displaying different nanowire structures.[34] In addition, Hasmy *et al.* have investigated the formation and stability of suspended Au, Ag, and Cu monatomic chains by using TBMD.[35] Single atomic chain formation has been observed at temperatures equal to or above 500, 200, and 4 K for Au, Ag, and Cu, respectively, and Ag and Cu form shorter chains compared to Au. They have argued that stability of chains is related to permanent *sd* hybridization along the chain. In contrast to previous theoretical and experimental studies, Sato *et al.*[36] have revealed that Cu suspended linear atomic chains are possible along [111], [110], and [100] directions from both theoretical and experimental investigations, and along with Amorim *et al.*[37] have studied both the formation and the breaking of Cu nanowires by performing realistic molecular-dynamics simulations of the Cu nanowires under stress along [111], [110], and [100] crystallographic directions and found that the Cu nanowires have been formed in all direction but the nanowires have been short compared to the Au case.

 ©2011 American Physical Society

Furthermore, in the case of Au, helical nanowires are formed under stress and these wires evolve to longer linear chain nanowires upon stretching.[38]

Mechanical, structural, and electronic properties as well as the growth and the formation of nanowires may be modified by the interaction with atomic or molecular species. These effects are verified from conductance measurements together with calculations.[39–42] Recently, Thijssen *et al.* have reported that longer Au, Ag, and Cu chains can be formed in the presence of an O atom.[43,44] Hence the formation and the stability of the Ag and Cu chains can be enhanced by an oxygen atom. They have claimed that the atomic oxygen rather than the molecular one incorporate into the Au chains. Conductance measurements exhibit a peak at $1G_0$ at both 4.2 and 40 K and a small peak at $0.1G_0$ at 40 K.[43] Besides, Zhang *et al.* have attended that the contaminated nanowires exhibit enhanced strength and tip atoms can join to the wire upon stretching by investigating the interaction of the tip suspended gold chains with molecular oxygen and dissociated oxygen.[45] The conductance of the wire containing molecular oxygen has been found to be close to $1G_0$, in agreement with the experimental results.[43] Moreover, the low conductance value as $0.1G_0$ observed in the experiment can be related to incorporation of an atomic oxygen into the Au nanowire. On the other hand, Novaes *et al.*[23] have demonstrated that the insertion of an oxygen atom in a thin gold nanowire can affect the breaking of the nanowire. The O atom forms both stable and strong bonds with the gold atoms in the nanowire and can mediate extraction of atoms from the tip to form longer chains. In addition, the formation of the monatomic gold chains in the presence of impurities (H, C, O, and S) have been simulated by Anglada *et al.*[46] They have observed that the hydrogen atom always evaporates before the formation of the chain and the C and O atoms can be incorporated into the chain, but with a low probability. However, the S atom is almost always found in the final stage of the chain. Also, the interaction of hydrogen molecule with gold nanojunction and nanowire have been studied. Csonka and co-workers.[47,48] have shown that the Au chains can be pulled even in a hydrogen environment and can interact strongly with the hydrogen molecules from experimental investigation of the interaction of the hydrogen molecule and the gold nanowire. However, the conductance of the clean gold chain drops to lower values in the presence of hydrogen molecule. Besides, the interaction of the H_2 and the gold nanowire strongly depend on the elongation stage of the nanowire.[49] The H_2 molecule can incorporate into the gold chain with a high binding energy and affects its conductance. Furthermore, Jelinek *et al.* have analyzed evolution of the mechanical and transport properties of the clean and contaminated Au nanowires during stretching.[50] Recently, simulation of the elongation of silver contact in the presence of the O_2 molecule and electronic transport during elongation have been calculated by Qi.[51] They have found that O_2 molecule can coalesce into the chain and affects the transport of the silver nanocontact. Moreover, the electronic band structure of the Au atomic nanowires has been modified and has been tuned by adjusting the density of the Si impurity atoms.[52]

A detailed investigation of the interaction of atomic and molecular species with nanocontacts and nanowires is essential for both fundamental and applied perspectives. In this paper, we have studied the stability, mechanical, and electronic properties of the clean and contaminated monatomic nanowires from first principles. After introducing the computational methods, infinite clean Au, Ag, and Cu nanowires have been presented. Next, the effect of impurity atoms, namely H, H_2, C, O, and O_2, on the stability, mechanical, and electronic properties of Au, Ag, and Cu monatomic chains has been discussed.

II. METHOD

We have performed first-principles plane-wave calculations[53,54] within density functional theory (DFT),[55] using ultrasoft pseudopotentials.[56] A plane-wave basis set with kinetic energy cutoff (E_{cut}) 400 and 560 eV has been used depending on the pseudopotentials of atoms. The exchange-correlation potential has been approximated by generalized gradient approximation (GGA) by using PW91 formulation.[57] All structures have been treated in a tetragonal supercell geometry (with lattice parameters a, b, and c) using periodic boundary conditions. In order to eliminate interaction between adjacent isolated wires, a large spacing ($a = b \sim 13$ Å) has been introduced. The nanowires have been oriented along the z axis. The Brillouin zone of the nanowires has been sampled by $1 \times 1 \times 49$ and $1 \times 1 \times 15$ **k**-point meshes within the Monkhorst-Pack scheme[58] for the unit cell and supercell containing four unit cells, respectively. Note that linear and zigzag structures contain one and two atoms in their unit cells, respectively. For partial occupancies, we have used the Methfessel-Paxton smearing method.[59] The width of smearing has been chosen as 0.05 eV for geometry optimization calculations. All atomic positions and lattice parameters have been optimized by using the conjugate gradient method where total energy and atomic forces have been minimized. The convergence for energy has been chosen as 10^{-5} eV between two ionic steps, and the maximum force allowed on each atom has been set to 0.03 eV/Å.

III. INFINITE WIRES

In this section, infinite linear and zigzag monatomic chains of Au, Ag, and Cu have been studied in order to provide a benchmark for the following calculations, and results have been compared with available experimental and theoretical works. Figure 1(a) shows the structures of these chain nanowires. Total energy of a given wire structure has been obtained by fixing both shape and lattice parameters of the structure, but the atoms within the unit cell are fully relaxed. Figure 2(a) displays the variation of the cohesive energy E_{coh} of clean monatomic wires of Au, Ag, and Cu as a function of d, which represents both the interatomic distance and the lattice constant (c) in the linear monatomic chains and half of the lattice constant in the zigzag chains. The definition of d is illustrated in Fig. 1(a). We have defined E_{coh} in terms of the calculated total energy of nanowire ($E_{\text{tot}}^{\text{wire}}$) and the spin polarized ground-state energy of the isolated metal atom (E_{atom}) composing the nanowire:

$$E_{\text{coh}} = \frac{E_{\text{tot}}^{\text{wire}}}{n} - E_{\text{atom}},$$

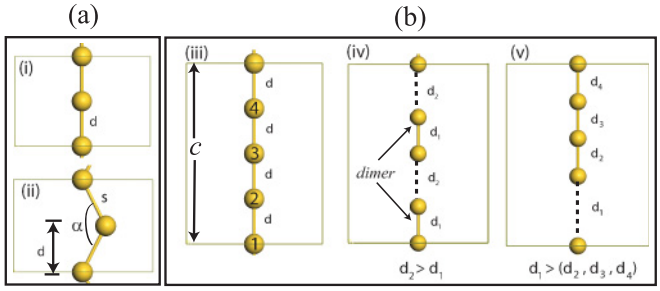

FIG. 1. (Color online) (a) Structure of (i) linear and (ii) zigzag monatomic chain nanowires. d and s are the interatomic distances in linear and zigzag wires, respectively. α is the bond angle defined for zigzag wire. In (b), unit-cell and structural properties of (iii) uniformly expanding, (iv) dimerized, and (v) broken wires are shown. In uniformly expanding wire case, d represents the common bond length and c is the lattice constant, which is always equal to $4d$. Dimerized wire can be described as a linear chain of dimers. d_1 and d_2 are the bond length in the dimer and dimer-dimer distance, respectively. In the broken wire case, wire splits into two weakly or noninteracting parts from a particular bond. d_1 is the distance between these two separated parts.

where n is the number of atom in the nanowire, and it is equal to 1 and 2 for the linear and the zigzag chains, respectively.

A common feature is that the zigzag structure is more energetically favorable than the linear one for all studied elements. The zigzag structure of Au has two minima. The structures at both of the minima are more stable than the linear

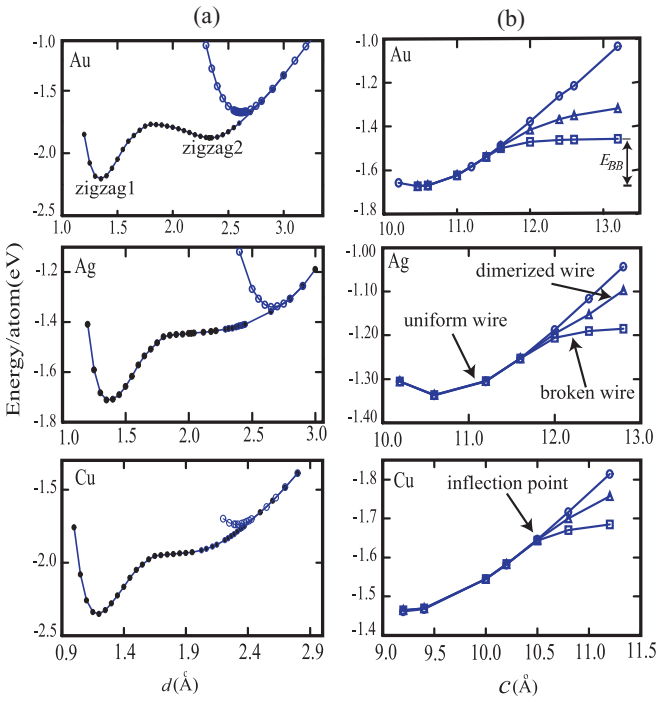

FIG. 2. (Color online) (a) Variation in the calculated cohesive energy E_{coh} as a function of d for infinite Au, Ag, and Cu monatomic chains. For zigzag chains, d is equal to half of the lattice constant. Open (solid) circles represent the linear (zigzag) structure. (b) Cohesive energy versus lattice constant variation in the uniformly expanding (open circles), the dimerized (triangle), and the broken wires (square).

structure. The calculated structural parameters and cohesive energies of all wires are summarized in Table I. It is well known that Au, Ag, and Cu atoms have eight first nearest neighbors in their bulk crystals, while the coordination number is only two for linear monatomic chain and at most three for the narrow angle zigzag chain. Because of this, the nearest-neighbor distances in nanowires are shorter than those in bulk crystal.

According to the well-known Peierls distortion, a uniform one-dimensional chain structure with a partially filled band cannot be stable, hence there are other structures like dimerized chain lower in energy compared to perfect chain structure. In this phenomena, a bond-length alternation occurs in the wire and the system undergoes a metal-to-insulator transition. The possibility of Peierls distortion and the mechanical stability has been investigated by stretching the clean monatomic chains along the wire axis. A four-atom supercell has been constructed for the linear nanowires of Au, Ag, and Cu. We have considered three different wire structures, which are labeled as uniformly expanding, dimerized, and broken wires, shown in Fig. 1(b). The variation in cohesive energy as a function of lattice constant (c) along the wire axis for these wire structures is displayed in Fig. 2(b). In all elongation steps, we have conserved the linearity of wire structure, that is, the relaxation of atoms has been allowed only along the wire direction. Here, we have observed three different behaviors. In the first one, the monatomic chain elongates uniformly under axial tensile force by preserving the symmetry, corresponding to uniformly expanding wires denoted in Fig. 1(b)(iii). However, this type of elongation is energetically favorable up to a certain lattice constant or elongation level. Beyond a critical point, which is different for each element, two different elongations of chains are likely to take place. This point represents the inflection point of the energy curve shown in Fig. 2(b). After this point, two different structural transformations of the nanowire might be observed, and a smaller force is required to pull the nanowire further. These two possible behaviors are called dimerization and breaking of the nanowire. In the former case depicted in Fig. 1(b)(iv), we have observed two different bond lengths, which are the interatomic distance in each individual dimer (d_1) and the dimer-dimer distance (d_2). d_1 approaches the equilibrium isolated dimer bond length as the distance between the dimers is long enough to eliminate interaction between them. In the case of the last possible elongation, one of the interatomic distance in the nanowire is very long compared to the others and wire breaks from this bond, displayed in Fig. 1(b)(v). The dimerized and breaking structures have been obtained by moving the second and third atoms of the uniformly expanding wire in opposite directions in small amounts. Then, system has been allowed to relax again. It is seen from Fig. 2(b) that the uniformly expanding structure is not energetically favorable after the inflection point. When the inflection point is reached, the sign of force changes from minus to plus, and wire begins to exhibit particular behaviors that are different from that of the uniformly expanding structure. The energy of the system is lower when the wire elongates irregularly; in other words, each bond expands in different amounts. The energy gain is larger than the energy loss upon the breaking of a bond for the broken structure. Two bonds must be broken in order to obtain the dimerized wire, while we need to break only one

TABLE I. Comparison of the calculated structural parameters and cohesive energies (E_{coh}) for the linear and the zigzag structures of Au, Ag, and Cu nanowires. The nearest-neighbor distance (d) and E_{coh} has also been calculated for the optimized bulk crystals. s and α are interatomic distance and bond angle in the zigzag nanowire, respectively. d_{max} and F_B represent the maximum possible nearest-neighbor bond length and the force (1 nN = 0.62 eV/Å) sustainable by the four-atom nanowire just before breaking, respectively. E_{BB} is the energy of broken bond.

Atom	Structure	d (Å)	s (Å)	α (deg)	E_{coh} (eV)	d_{max} (Å)	F_B (nN)	E_{BB} (eV)
	linear	2.62	2.62	180	1.67	2.90	1.79	0.87
Au	zigzag1	1.35	2.75	58.8	2.20			
	zigzag2	2.34	2.57	130.6	1.87			
	bulk	2.95			3.21			
	dimer	2.53			1.29			
	linear	2.67	2.67	180	1.34	2.90	1.06	0.61
Ag	zigzag	1.35	2.80	57.7	1.71			
	bulk	2.93			2.76			
	dimer	2.58			1.06			
	linear	2.30	2.30	180	1.74	2.63	1.53	0.89
Cu	zigzag	1.20	2.41	59.7	2.36			
	bulk	2.58			3.76			
	dimer	2.22			1.33			

bond for forming the broken wire. Therefore the energy gain in the formation of the dimerized wire is lower than that of the broken wire. As a result, the wire prefers to break after the inflection point. We can estimate the energy of the broken bond (E_{BB}) by simply taking the difference between equilibrium structure total energy of uniformly expanding wire and the total energy of the completely broken wire. The total energy does not change anymore upon pulling the nanowire in the broken structure. Table I shows the breaking point (d_{max}), the breaking force (F_B), and the broken bond energy in the breaking wire. F_B and d_{max} are the maximum force sustainable by nanowire just before the rupture and the maximum possible bond length, respectively. It is found that F_B takes the highest value in the Au wire case. The calculated F_B values for Au, Ag, and Cu are 1.79, 1.06, and 1.53 nN, respectively. Bahn and Jacobsen[30] have calculated the breaking forces of Au, Ag, and Cu chains as 1.31, 0.9, and 1.18 nN, respectively. The experimental value of F_B for Au chain is 1.5 ± 0.3 nN,[60] in agreement with our results. Rubio-Bollinger *et al.*[60] have calculated F_B ranging from 1.6 to 1.7 nN by using GGA. They have pointed out that the value of F_B depends on the exchange-correlation functional. da Silva and co-workers[8,9] have studied the formation, evolution, and breaking of Au nanowires from DFT based methods. They have found F_B as 2.4 nN for LDA and 1.9 nN for GGA. Ribeiro and Cohen[61] have obtained a value of 2.5 nN by using LDA. The breaking force of 1.75 nN has been found by Ayuela *et al.*[29]

Ag nanowire has both the smallest broken bond energy and the smallest breaking force. Cu and Au have very similar bond energies being 0.87 and 0.89 eV, respectively. The longest interatomic bond distances in the four-atom-long Au chain just before breaking is found to be 2.9 Å. In literature, one of the longest Au-Au bond distances before rupture of wire is around 3.1 Å.[8,9,29] Skurodumova *et al.*[62] have studied the electronic structure and the stability of gold nanowires of different lengths. They have shown that the wire stability steadily decreases with increasing number of atoms (N) in the supercell. When $N = 2$ and 3, the breaking point is close to 2.9 Å. This bond distance decreases to 2.6 Å, when $N \geqslant 7$. The $N = 4$ case is similar to our case. When the Au-Au bond length exceeds the value of 2.9 Å, breaking is more favorable than dimerization.

IV. EFFECT OF THE IMPURITY

Next, we have investigated the effect of impurity atoms (H, C, and O) and molecules (H_2 and O_2) on the electronic properties and the mechanical stability of Au, Cu, and Ag monatomic chains. The wire structures used in calculations are represented in Fig. 3(a). The wire-impurity system has been put in a large tetragonal supercell to get rid of interactions among the wire-impurity system and its periodic images. We have thoroughly checked the effect of cell size along the wire axis, i.e., periodic direction, on Au_n-C ($n = 2,3,4,5,7$) wires. For longer chains, the only significant change is the length of the metal-metal bond farthest away from the impurity atom, and it approaches to the value of the bond length of the pure metal wire, while the corresponding energy change in pure chain wire is just 20 meV. In experiments, nanowires are finite in length and form between two tips. Previous studies[63,64] have suggested that the stability of a nanocontact containing a monatomic chain is mainly determined by its chain part. Therefore our simple model is reliable to study stability of both clean and contaminated monatomic chains. Experimentally, most of the nanowires are created under tension. Therefore we have also considered nanowires under tension to simulate realistic experimental conditions. The wire-impurity system has been elongated with a small increment, $\Delta c = 0.2$ Å, and all atoms have been allowed to relax. We have kept the linear structure of the nanowires during structural optimization. At each step, the total energy of the system has been recalculated. The relaxed previous step has been used as the initial structure of the next step. This procedure has been continued until the nanowire rupture.

It is expected that the breaking of a contaminated nanowire should be different than that of a clean one due to the presence of the impurity; the impurity should modify the strength and

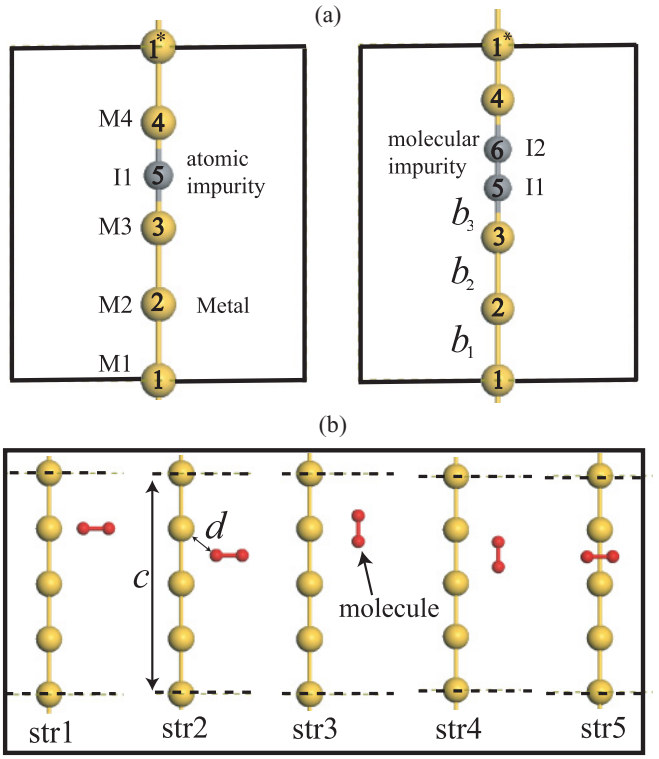

FIG. 3. (Color online) (a) Impurity inserted in the linear monatomic chain. Big yellow (small gray) spheres represents metal (atomic or molecular impurity). Distances between the relevant atoms at equilibrium are given in Table II. Metal atoms have been labeled as M1, M2, M3, and M4. I and I1-I2 represent the atomic and molecular impurities, respectively. (b) Possible interaction configurations of molecular impurity with the clean nanowire.

stability of the bonds. Consequently, we have studied the broken bond energies of the metal-metal bond far away from the impurity (the bond between M1 and M2), the metal-metal bond just next to the impurity (M2-M3), and the metal-impurity bond (M3-I1). Several structural parameters for the equilibrium structures, the broken bond energies for several bonds, and the position of the broken bonds are summarized in Table II. Which bond breaks first during the elongation strongly depends on the type of impurity. Except Ag-O and -C wires, the breaking of the bond b_1 is energetically more favorable compared to the other bonds in the atomic impurity case, implying that the impurity has an influence not only on the first-nearest-neighbor but also on the next-nearest-neighbor metal atoms and bonds. Figure 4 displays the evolution of the bond lengths for the atomic impurity as a function of the elongation. We have observed that the metal-impurity bond (b_3) length remains almost constant during stretching. On the other hand, the length of the metal-metal bonds (b_1 and b_2) increases almost linearly up to a certain lattice constant. The rupture of nanowire immediately happens beyond this critical wire length and a sharp variation in the bond lengths occurs.

Similar to the clean nanowire case, broken bond energy has been defined in terms of the calculated total energy of the equilibrium structure of the contaminated nanowire $E_{\rm tot}^{GS}$ and the total energy of the corresponding completely broken structure ($E_{\rm tot}^{BS}$) as $E_{\rm tot}^{BS} - E_{\rm tot}^{GS}$. The broken bond energy reflects the stiffness of a particular bond. In Table II, we have given three different broken bond energies, namely E_{BB}, E_{BB}^{23}, and E_{BB}^{35}. E_{BB} is the broken bond energy of the weakest bond. E_{BB}^{23} (E_{BB}^{35}) denotes the broken bond energy of the bond that is between M2 and M3 (M3 and I1). E_{BB} takes the highest value in the H case and it is lower than E_{BB} of clean nanowires; see Tables I and II. The incorporation of the atomic impurity weakens the strength of the bond b_1. In the atomic impurity case, E_{BE}^{35} is at least 1.5 times larger than E_{BB}. We have found that the Au, Cu, and Ag nanowires contaminated with O and H never break from the M-I bond. E_{BB} takes noticeably small values in the molecular impurity cases. We can suggest that the formation of linear Ag-H_2 and Ag-O_2 monatomic chains illustrated in Fig. 3(a) is not possible according to our model. However, the Cu-O_2 system is quite stable compared to Ag and Au wires containing H_2 and O_2 molecules.

In the molecular impurity cases, the O-O and H-H bond distances can help to quantify the interaction strength between the molecules and the nanowires. In the isolated O_2 and H_2 molecules, the bond distances are calculated as 1.23 and 0.74 Å, respectively. The O-O bond length becomes 1.28 Å for Au, 1.31 Å for Cu, and 1.27 Å for the Ag case. The highest stretching in the O-O bond has been achieved in the Cu nanowire, implying that interaction between the O_2 molecule and the Cu chain is the strongest one. For the H_2 molecule case, the H-H bond length increases to 0.87, 0.85, and 0.8 Å for Au, Cu, and, Ag, respectively. Both molecules do not dissociate over the nanowires. Similarly, Jelinek *et al.* have shown that the energy barrier for the H_2 dissociation over the stretched Au nanowire is 0.1 eV.[50] Moreover, Barnett *et al.* have shown that a barrierless incorporation of H_2 into the nanocontact is possible for the broken Au wire.[49]

The Bader charges[65,66] have been calculated for equilibrium structures and are tabulated in Table III. We have observed that charge transfers from metal atoms to the impurity. The Bader analysis reveals that O takes more charge from the nanowire compared to C and H atoms. While the calculated Bader charge on the C (H) atom is in the range -0.23 $(-0.06)|e|$ to -0.41 $(-0.29)|e|$, the Bader charge on the O atom in the nanowire is in the range $-0.65|e|$ to $-0.83|e|$. This is expected since O is the most electronegative element among the studied impurities. The metal atoms on the either side of the atomic impurity are always positively charged, ranging from $+0.17|e|$ to $+0.45|e|$. The charge on metal atoms M1 and M2 is usually small compared to that on M3 and M4 atoms.

The character of the bonds in the Cu-atomic impurity nanowire is displayed as a prototype in Fig. 5 using charge-density contour plots. The Au and Ag wires exhibit similar properties. The covalent character of the Cu-C bond is depicted by the localization of bond charge between Cu and C atoms. However, in the Cu-H and the Cu-O nanowires, ioniclike bonding is observed between the metal and the impurity atoms. The presence of the impurity atoms modifies the charge distribution along the nanowire. Due to the covalent nature of the Cu-C bond, impurity-metal bond energy takes the highest value in the Cu-C nanowire; see Table II. Due to the character of the bonds, the Cu-H and Cu-O bonds are more flexible compared to the Cu-C bond.

TABLE II. Optimized bond lengths between the relevant atoms d_{ij} (in Å) for equilibrium structures. E_{BB} is the energy of the weakest bond and BB indicates the position of this bond in terms of the labeled atoms i and j. E_{BB}^{35} and E_{BB}^{23} are the metal-impurity (M1-I) and metal-metal (M2-M3) bond energies, respectively. F_{break}^{np} is the breaking force of M1-M2-M3-I-M4 nanowire. Breaking force of M-I alloy nanowire is denoted by F_{break}^{p}. Forces are given in units of nN (= 0.62 eV/Å). μ is the net magnetic moment per cell in units of Bohr magneton (μ_B). EP means electronic properties of nanowires. S and M stand for metallic and semiconducting nanowire. The values quoted in parentheses are the energy band gaps for semiconducting nanowires. Energies are given in eV.

System	d_{12}	d_{23}	d_{34}	d_{35}	E_{BB}	BB	E_{BB}^{35}	E_{BB}^{23}	F_{break}^{np}	F_{break}^{p}	μ	EP
Au-H	2.59	2.61	3.32	1.66	0.87	1-2	1.34	1.19	1.56	2.92	0	M
Au-H_2	2.66	2.59	4.36	1.74	0.30	3-5	0.30	1.17			0	S (0.32)
Au-C	2.63	2.52	3.74	1.87	0.47	1-2	2.80	1.73	0.90	4.84	0	S (0.13)
Au-O	2.65	2.52	3.92	1.96	0.55	1-2	1.39	1.67	1.16	4.21	2	M
Au-O_2	2.67	2.53	5.66	2.19	0.16	3-5	0.16	1.88			2	S(0.68)
Ag-H	2.65	2.68	3.44	1.72	0.83	1-2	1.36	0.97	1.01	2.27	0	M
Ag-H_2	2.70	2.62	4.76	1.98	0.17	3-5	0.17	1.15			0	S(0.6)
Ag-C	2.77	2.69	4.06	2.03	0.68	2-3	1.53	0.68	0.85	2.77	1.73	M
Ag-O	2.66	2.68	4.11	2.06	0.72	2-3	1.34	0.72	1.00	2.97	1.74	M
Ag-O_2	2.70	2.60	6.19	2.43	0.03	3-5	0.03	1.42			2	M
Cu-H	2.31	2.31	3.08	1.54	0.87	1-2	1.48	1.26	1.34	2.71	0	M
Cu-H_2	2.34	2.28	4.19	1.68	0.37	3-5	0.37	1.34			0	S(0.32)
Cu-C	2.31	2.30	3.58	1.79	0.74	1-2	2.54	1.29	1.03	4.35	0.94	M
Cu-O	2.33	2.30	3.53	1.77	0.65	1-2	2.18	1.41	1.05	4.77	2	M
Cu-O_2	2.34	2.23	4.94	1.81	0.53	1-2	0.72	2.07			2	S(0.21)

As listed in Table II, except for the Au-C system, magnetism emerges in wires containing C, O, and O_2 impurities whereas the clean Au, Ag, and Cu chains have nonmagnetic ground state. C and O have valence electronic configurations of s^2p^2 and s^2p^4, respectively. In the Cu-impurity system, p orbitals of both C and O atoms contribute the formation of magnetic ground state. Local magnetic moments on O and C are $0.545\mu_B$ and $0.43\mu_B$, respectively. For the Cu-O case, the sum of the local magnetic moments on Cu atoms is calculated as $1.03\mu_B$. Magnetization is affected from elongation of the nanowire. For example, the total magnetic moment in the Ag-C system is $1.64\mu_B$ at $c = 10.8$ Å and becomes $1.83\mu_B$ at $c = 12.8$ Å.

We have also considered the linear alloy nanowires of Au, Ag, and Cu with O, C, and H for comparison. These types of nanowires have two atoms in their unit cells with metal-impurity periodic units. Applied force on the alloy nanowires calculated at each lattice constant is given as $F_z = \frac{\partial E_T}{\partial \Delta z}$, where Δz is the amount of elongation of the nanowires. Breaking force (F_{break}^{p}) of these alloy nanowires is higher than 2.77 nN for O and C cases and in the range 2.27–2.92 nN for H; see Table II for the list. The Au-C nanowire has the highest F_{break}^{p}, which is found to be 4.84 nN. These force values are relatively high compared to breaking forces (F_{break}^{np}) of the M1-M2-M3-I-M4 nanowires illustrated in Fig. 3, because we have calculated F_{break}^{p} with two atoms unit cells. Another important point is that alloy nanowires have only metal-impurity bonds, which are quite strong compared to metal-metal bonds. We can consider these F_{break}^{p} values as the upper theoretical limit for the breaking force of Au, Ag, and Cu wires containing atomic impurities. Note that F_{break}^{np} values for atomic impurities only are presented in Table II. There is a strong correlation between E_{BB} and F_{break}^{np}. Both of them follow the same trend. For each metal atom, the highest F_{break}^{np} value has been obtained for the wire containing the H atom. We have observed that F_{break}^{np} values are smaller than F_B of the clean monatomic chains. Although the impurity atoms strongly bind to the nanowires and form strong bonds with the metal atoms, they usually cause weakening of the farthest metal-metal bond. While the breaking force or F_B of the clean Cu nanowire is 1.53 nN, it becomes 1.05 nN for Cu nanowire contaminated with O. It has been found that H (C) has the lowest (highest) effect on the breaking force. Insertion of C significantly reduces the breaking force of the Au wire. The maximum sustainable force just before nanowire rupture decreases from 1.79 nN (F_B of the clean Au nanowire) to 0.90 nN (F_{break}^{np} of the Au-C nanowire). Likewise, Skorodumova *et al.*[63] have calculated the breaking force of the infinite and finite Au_NC (and H) chains, where N represents the number of Au atoms in the unit cell of the infinite wires and the monatomic part of the tip supported finite nanowire. They have found similar breaking forces for the infinite and finite monatomic nanowires. For the infinite Au_4C (Au_4H) nanowire, the breaking force is calculated as 1.0 (1.6) nN, in agreement with our findings. The calculated value of F_{break}^{np} is 0.90 nN for C and 1.56 nN for the H impurity case.

In order to get more insight about the interaction of nanowire with the impurities, we have also considered gas phase H_2 and O_2 molecules as displayed in Fig. 3(b). Concerning the lowest energy configuration, we have considered five configurations with different orientation of the H_2 and O_2 molecules. The initial distance of impurity from the nanowire varies between 2 and 2.45 Å. We have chosen two different lattice constants c for each system. These are $c = 9.92$ (2.48) Å and 10.2 (2.55) Å for Cu chains, and 11.12 (2.78) Å and 11.4 (2.85) Å for Au and Ag nanowires. The values given in parentheses are the average interatomic distances in clean nanowires for the given lattice constants.

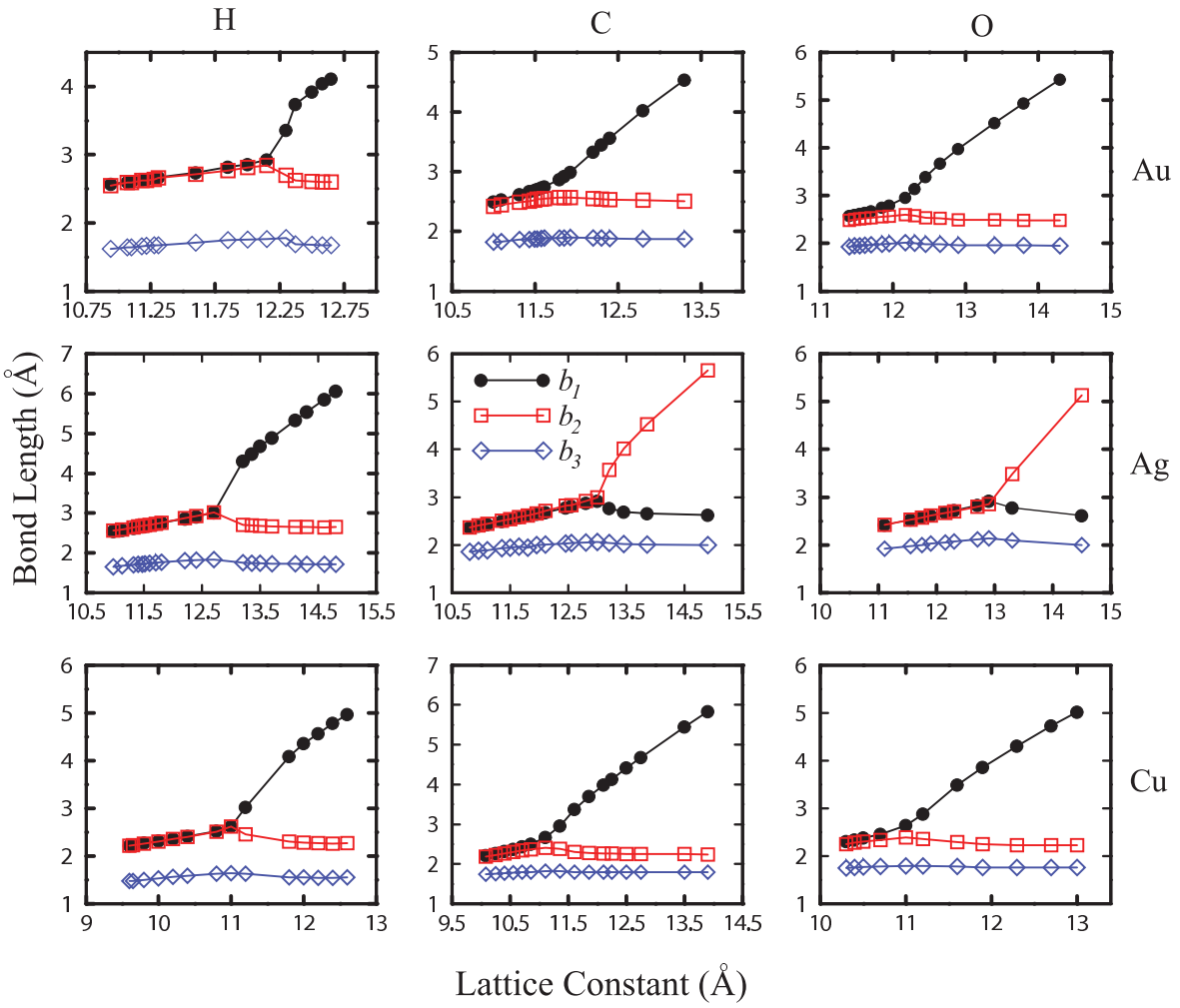

FIG. 4. (Color online) Variation in the bond lengths during stretching of chain nanowires. The bond lengths b_1, b_2, and b_3 are represented by solid circles, open squares, and open diamonds, respectively.

At these lattice constants, the linear structure is energetically more favorable than the zigzag structure.

In general, the Ag nanowire does not interact with the molecular species. H_2 and O_2 molecules are repelled by the Ag nanowire. Therefore only the physisorbed state might be possible. Remember that the linear Ag-molecular impurity system is very brittle against elongation and the energy of bond b_3 is very small compared to the one in the atomic impurity cases. As a result of elongation, wire breaks from bond b_3; see Table II. The Cu nanowire forms strong chemical bonds with the O_2 in all configurations for both lattice constants. The initial linear structure of the nanowire turns into a distorted zigzag structure upon interaction with the impurity. However, the H_2 molecule strongly interacts with the nanowire and incorporates into the Cu chain only in **str4** for $c = 11.4$ Å and **str5** for both c values. On the other hand, the Au nanowire strongly attracts the O and H molecules in **str2**, **str4**, and **str5** for $c = 11.4$ Å. Meanwhile, for the other c value, interaction is

TABLE III. The calculated Bader charge on each atom in the atomic impurity cases for equilibrium structures. + (−) means that charge is given (taken).

	Au			Ag			Cu		
Atom	O	C	H	O	C	H	O	C	H
M1	−0.05	−0.22	−0.05	+0.05	−0.04	−0.12	+0.005	−0.057	−0.06
M2	−0.13	−0.17	−0.05	−0.004	+0.02	−0.12	−0.05	−0.055	+0.01
M3	+0.45	+0.28	+0.08	+0.40	+0.23	+0.17	+0.44	+0.28	+0.18
I	−0.65	−0.23	−0.06	−0.75	−0.41	−0.1	−0.83	−0.39	−0.29
M4	+0.38	+0.34	+0.08	+0.40	+0.22	+0.17	+0.43	+0.23	+0.18

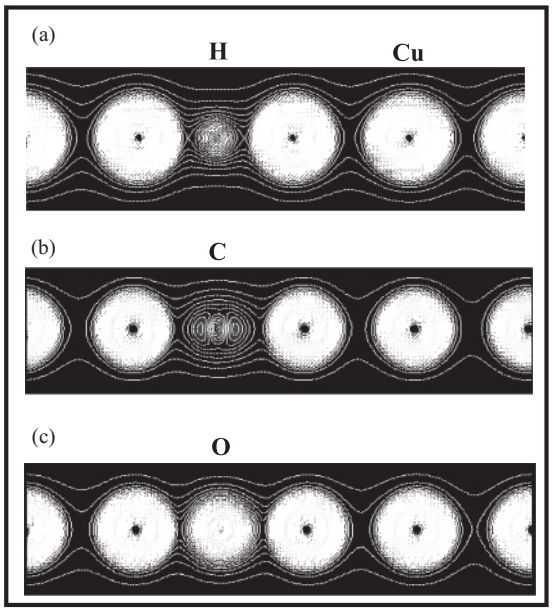

FIG. 5. Charge-density plots of (a) Cu-H, (b) Cu-C, and (c) Cu-O nanowires on a plane passing through the bonds.

weak. It can be argued that there is a close relation between the interaction strength and the length of the nanowire. The initial structure and the lattice constant considerably influence the interaction between the nanowire and the impurity. The Au and Cu nanowires show higher reactivity to H_2 and O_2 molecules compared to the Ag nanowire.

Next, we have studied the breaking dynamics of wire-impurity systems by simply applying tensile stress along the wire direction. We have started with the relaxed structures of **str4** wire depicted in Fig. 3(b) for the contaminated Cu and Au nanowires. The wires have been elongated in small steps of 0.1, 0.15, and 0.2 Å depending on the type of impurity and metal atoms. At each step of elongation, the wire has been allowed to relax and this relaxed structure of the previous step has been used as the initial structure of the next step. The evolution of the Cu-O_2 nanowire can be followed from Fig. 6(a). The utmost bond length stretching is observed between Cu(1) and Cu(2) atoms. At the strain value of 11.6%, the Cu(1)-Cu(2) bond length increases from 2.31 to 3.47 Å. However, the O-Cu bond length stays almost constant during pulling. The O-O bond significantly elongates (about 0.12 Å), verifying the strong interaction existing between the Cu nanowire and oxygen molecule. The wire tends to break when c exceeds

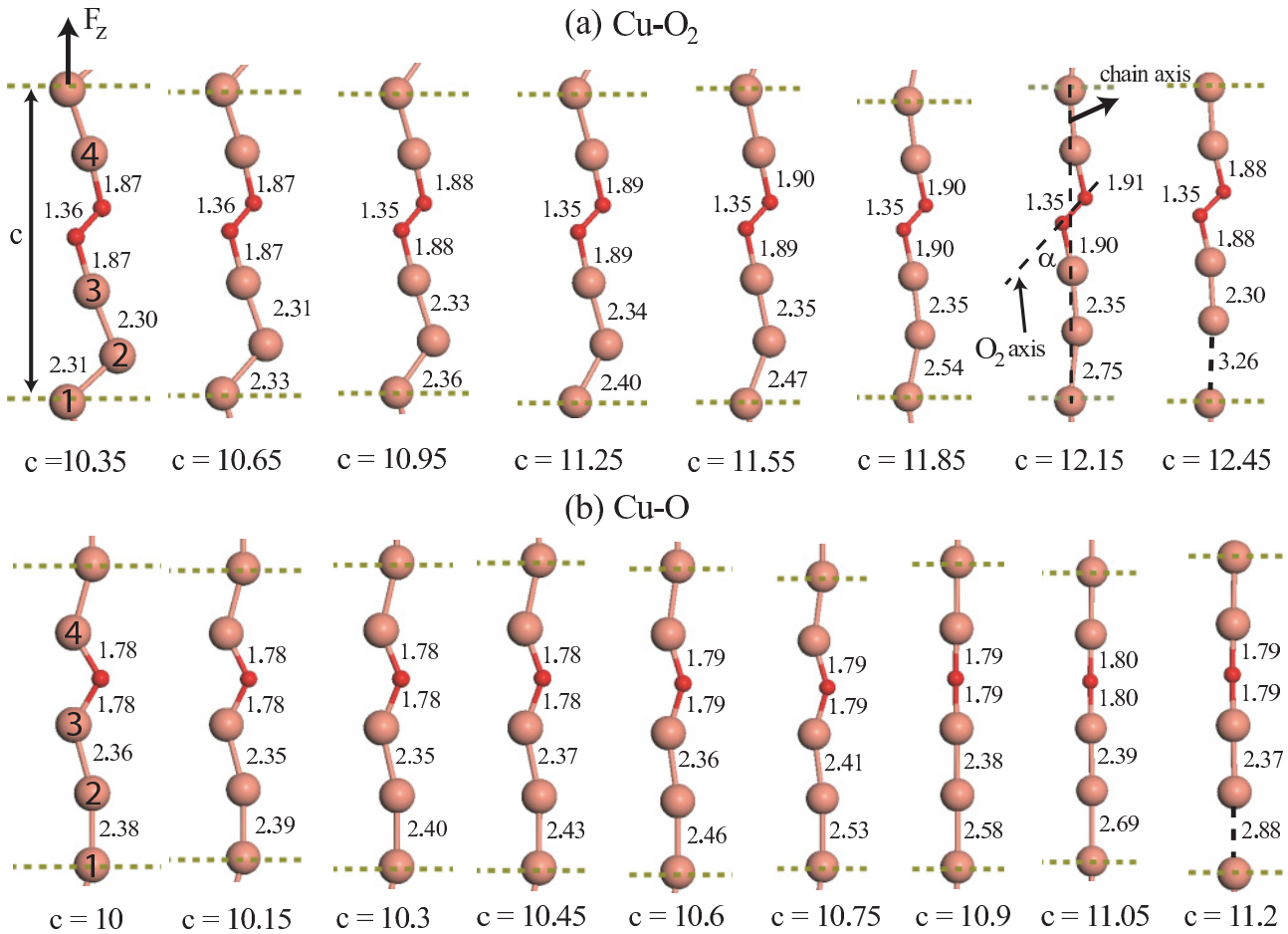

FIG. 6. (Color online) Snapshots of structural evolution of the **str4** in (a) Cu-O_2 and in (b) Cu-O during the stretching. Lattice constants c (in Å) and bond lengths (in Å) between the relevant atoms are shown. Big pink (small red) spheres represent Cu (O) atoms. Chain axis denoted by dashed line is parallel to the z direction. We have also defined an axis for O_2 molecule, passing through O atoms. α is the angle between chain axis and molecule axis.

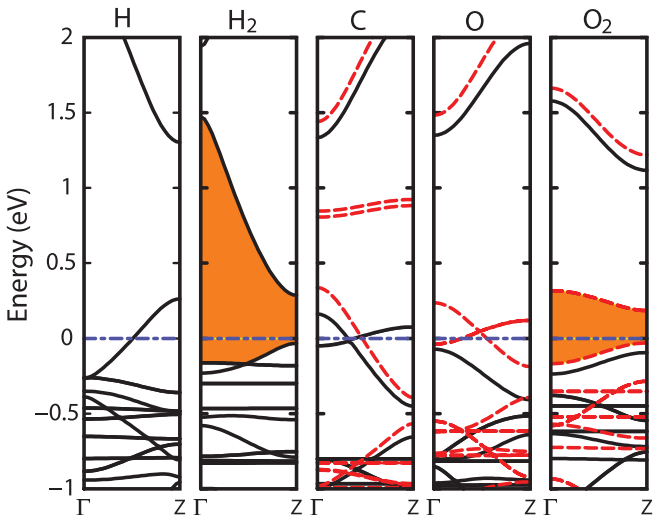

FIG. 7. (Color online) The band structure of Cu-H, Cu-H_2, Cu-C, Cu-O, and Cu-O_2. Fermi level of metallic systems shown by dashed lines marks the zero of energy. In semiconducting wires, the zero of the energy indicates the top the valence band. For magnetic systems, majority (minority) spin components are represented with dark solid (red dashed) lines.

11.85 Å. This value is comparable with the breaking point of the linear Cu-O_2 wire. The maximum force sustainable by the nanowire just before rupture is found to be 1.05 nN. Interestingly, total magnetic moment ($2\mu_B$) of the wire does not change during stretching. The axis passing through O atoms does not coincide with the axis of the nanowire in any step. While the orientation of the O_2 molecule changes slightly, Cu atoms move to the chain axis during the pulling. The wire-molecular impurity system usually breaks before complete linearization is obtained. However, in the case of Cu-atomic oxygen impurity depicted in Fig. 6(b), the structure of the wire becomes linear before the nanowire breaking. All atoms almost line up on the chain axis and the wire eventually breaks from the Cu-Cu bond remote from the impurity. Due to the interesting behavior of the Cu-oxygen system explained above, we can claim that long and stable Cu monatomic chains may form in an oxygen-rich environment. Our findings are in agreement with the recent experimental results, which have shown that the presence of oxygen induces the formation of long Cu-O chains.[43]

Electronic properties of the wire-impurity systems are outlined in Table II. The Au-O and Cu-O systems exhibit half metallic behavior. These chains are metallic for one spin direction while they are semiconducting for the other spin direction. Majority spin components have an energy gap of 1 eV for Au and 1.3 eV for Cu case. Except Ag-O_2, wire-molecular impurity systems display semiconducting character. E_g is in the range 0.13–0.68 eV. Interestingly, the Au-C nanowire is a semiconductor with a gap of 0.13 eV in agreement with the findings of Skorodumova *et al.*[63] Moreover, they have observed conductance oscillations in C and H contaminated Au nanowires as a function of the number of Au atoms (N). It has been shown that there is a single band crossing the Fermi level if the Au-C and Au-H chains contain an odd and even number of Au atoms N, respectively. In our work, we have considered even N chains, and Au-C and Au-H systems show semiconducting and metallic behaviors, respectively. In Fig. 7, only the band structures for Cu case are shown as a prototype. For metallic systems, bands crossing the Fermi level have d- and p-orbital character in Cu-O and Cu-C systems. In the H case, both s and p orbitals of Cu atoms contribute to the metallic band crossing the Fermi level. Since C (and also O) provides an additional four (two) valent p electrons to the nanowire system, incorporation of these impurities significantly modifies the electronic structure of the clean wire.

V. CONCLUSION

Interaction of atomic or molecular species with metal nanowires has been studied. We have found that atomic impurities interact more strongly with the nanowires compared to molecular ones. Impurity atoms can easily incorporate into the nanowires from the environment. The addition of an impurity remarkably modifies both mechanical stability and electronic properties of the clean nanowires. In general, the contaminated nanowires tend to break from a metal-metal bond remote from the impurity. Our findings suggest that the stability and electronic properties of the metal nanowires can be tuned by using appropriate doping. The presence of the suitable atomic and molecular impurities in the growth conditions can facilitate the formation of a stable nanowire of an element that has little tendency for the nanowire formation.

ACKNOWLEDGMENTS

Computing resources used in this work were provided by the National Center for High Performance Computing of Turkey (UYBHM) under Grant No. 10362008. Part of the calculations have been carried out at ULAKBIM Computer Center (TÜBİTAK). O.G. acknowledges the support of Turkish Academy of Sciences, TÜBA.

*Present address: Faculty of Science and Technology and MESA+ Institute for Nanotechnology, University of Twente, P.O. Box 217, 7500 AE Enschede, The Netherlands.
†gulseren@fen.bilkent.edu.tr

[1]N. Agräit, A. Levy-Yeyati, and J. van Ruitenbeek, Phys. Rep. **377**, 81 (2003).
[2]T. Kizuka, Phys. Rev. B **77**, 155401 (2008).
[3]H. Ohnishi, Y. Kondo, and K. Takayanagi, Nature (London) **395**, 780 (1998).
[4]A. I. Yanson, G. R. Bollinger, H. E. van der Brom, N. Agraït, and J. M. van Ruitenbeek, Nature (London) **395**, 783 (1998).
[5]M. Okamoto and K. Takayanagi, Phys. Rev. B **60**, 7808 (1999).
[6]L. De Maria and M. Springborg, Chem. Phys. Lett. **323**, 293 (2000).

[7]N. V. Skorodumova and S. I. Simak, Comput. Mater. Sci. **17**, 178 (2000).
[8]E. Z. da Silva, A. J. R. da Silva, and A. Fazzio, Phys. Rev. Lett. **87**, 256102 (2001).
[9]E. Z. da Silva, F. D. Novaes, A. J. R. da Silva, and A. Fazzio, Phys. Rev. B **69**, 115411 (2004).
[10]J. Nakamura, N. Kobayashi, and M. Aono, Riken Rev. **37**, 17 (2001).
[11]P. Velez, S. A. Dassie, and E. P. M. Leiva, Chem. Phys. Lett. **460**, 261 (2008).
[12]D. Sanchez-Portal, E. Artacho, J. Junquera, P. Ordejon, A. Garcia, and J. M. Soler, Phys. Rev. Lett. **83**, 3884 (1999).
[13]D. Sanchez-Portal, E. Artacho, J. Junquera, A. Garcia, and J. M. Soler, Surf. Sci. **482-485**, 1261 (2001).
[14]H. Koizuma, Y. Oshima, Y. Kondo, and K. Takayanagi, Ultramicroscopy **88**, 17 (2001).
[15]H. Hakkinen, R. N. Barnett, and U. Landman, J. Phys. Chem. B **103**, 8814 (1999).
[16]S. R. Bahn, N. Lopez, J. K. Norskov, and K. W. Jacobsen, Phys. Rev. B **66**, 081405 (2002).
[17]S. B. Legoas, D. S. Galvao, V. Rodrigues, and D. Ugarte, Phys. Rev. Lett. **88**, 076105 (2002).
[18]N. V. Skorodumova and S. I. Simak, Phys. Rev. B **67**, 121404 (2003).
[19]N. V. Skorodumova and S. I. Simak, Solid State Commun. **130**, 755 (2004).
[20]F. D. Novaes, A. J. R. da Silva, E. Z. da Silva, and A. Fazzio, Phys. Rev. Lett. **90**, 036101 (2003).
[21]F. D. Novaes, E. Z. da Silva, A. J. R. da Silva, and A. Fazzio, Surf. Sci. **566-568**, 367 (2004).
[22]S. B. Legoas, V. Rodrigues, D. Ugarte, and D. S. Galvao, Phys. Rev. Lett. **93**, 216103 (2004).
[23]F. D. Novaes, A. J. R. da Silva, E. Z. da Silva, and A. Fazzio, Phys. Rev. Lett. **96**, 016104 (2006).
[24]H. Zhai, B. Kiran, and L. Wang, J. Chem. Phys. **121**, 8231 (2004).
[25]E. Hobi Jr., A. Fazzio, and A. J. R. da Silva, Phys. Rev. Lett. **100**, 056104 (2008).
[26]A. E. Kochetov and A. S. Mikhaylushkin, Eur. Phys. J. B **61**, 441 (2008).
[27]P. Velez, S. A. Dassie, and E. P. M. Leiva, Phys. Rev. B **81**, 125440 (2010).
[28]C. Untiedt, A. I. Yanson, R. Grande, G. Rubio-Bollinger, N. Agraït, S. Vieira, and J. M. van Ruitenbeek, Phys. Rev. B **66**, 085418 (2002).
[29]A. Ayuela, M. J. Puska, R. M. Nieminen, and J. A. Alonso, Phys. Rev. B **72**, 161403(R) (2005).
[30]S. R. Bahn and K. W. Jacobsen, Phys. Rev. Lett. **87**, 266101 (2001).
[31]A. Thiess, Y. Mokrousov, S. Blügel, and S. Heinze, Nano Lett. **8**, 2144 (2008).
[32]R. H. M. Smit, C. Untiedt, A. I. Yanson, and J. M. van Ruitenbeek, Phys. Rev. Lett. **87**, 266102 (2001).
[33]F. Tavazza, A. Hasmy, L. E. Levine, A. M. Chaka, L. Rincon, M. Marquez, and C. Gonzales, e-print arXiv:cond-mat/0703313 (to be published).
[34]F. Tavazza, L. E. Levine, and A. M. Chaka, Phys. Rev. B **81**, 235424 (2010).
[35]A. Hasmy, L. Rincón, R. Hernández, V. Mujica, M. Márquez, and C. González, Phys. Rev. B **78**, 115409 (2008).
[36]F. Sato, A. S. Moreira, J. Bettini, P. Z. Coura, S. O. Dantas, D. Ugarte, and D. S. Galvão, Phys. Rev. B **74**, 193401 (2006).
[37]E. P. M. Amorim, A. J. R. da Silva, A. Fazzio, and E. Z. da Silva, Nanotechnology **18**, 145701 (2007).
[38]E. P. M. Amorim and E. Z. da Silva, Phys. Rev. Lett. **101**, 125502 (2008).
[39]T. Frederiksen, M. Paulsson, and M. Brandbyge, J. Phys.: Conf. Ser. **61**, 312 (2007).
[40]H. Ishida, Phys. Rev. B **75**, 205419 (2007).
[41]H. Ishida, Phys. Rev. B **77**, 155415 (2008).
[42]M. Kiguchi, T. Nakazumi, K. Hashimoto, and K. Murakoshi, Phys. Rev. B **81**, 045420 (2010).
[43]W. H. A. Thijssen, D. Marjenburgh, R. H. Bremmer, and J. M. van Ruitenbeek, Phys. Rev. Lett. **96**, 026806 (2006).
[44]W. H. A. Thijssen, M. Strange, J. M. J. aan de Brugh, and J. M. van Ruitenbeek, New J. Phys. **10**, 033005 (2008).
[45]C. Zhang, R. N. Barnett, and U. Landman, Phys. Rev. Lett. **100**, 046801 (2008).
[46]E. Anglada, J. A. Torres, F. Yndurain, and J. M. Soler, Phys. Rev. Lett. **98**, 096102 (2007).
[47]Sz. Csonka, A. Halbritter, G. Mihály, E. Jurdik, O. I. Shklyarevskii, S. Speller, and H. van Kempen, Phys. Rev. Lett. **90**, 116803 (2003).
[48]Sz. Csonka, A. Halbritter, and G. Mihály, Phys. Rev. B **73**, 075405 (2006).
[49]R. N. Barnett, H. Hakkinen, A. G. Scherbakov, and U. Landman, Nano Lett. **4**, 1845 (2004).
[50]P. Jelinek, R. Perez, J. Ortega, and F. Flores, Phys. Rev. B **77**, 115447 (2008).
[51]Y. Qi, D. Guan, Y. Jiang, Y. Zheng, and C. Liu, Phys. Rev. Lett. **97**, 256101 (2006).
[52]W. H. Choi, P. G. Kang, K. D. Ryang, and H. W. Yeom, Phys. Rev. Lett. **100**, 126801 (2008).
[53]M. C. Payne, M. P. Teter, D. C. Allen, T. A. Arias, and J. D. Joannopoulos, Rev. Mod. Phys. **64**, 1045 (1992).
[54]Numerical computations have been carried out by using VASP software: G. Kresse and J. Hafner, Phys. Rev. B **47**, R558 (1993); G. Kresse and J. Furthmüller, *ibid.* **54**, 11169 (1996).
[55]W. Kohn and L. J. Sham, Phys. Rev. **140**, A1133 (1965); P. Hohenberg and W. Kohn, *ibid.* **136**, B864 (1964).
[56]D. Vanderbilt, Phys. Rev. B **41**, R7892 (1990).
[57]J. P. Perdew, J. A. Chevary, S. H. Vosko, K. A. Jackson, M. R. Pederson, D. J. Singh, and C. Fiolhais, Phys. Rev. B **46**, 6671 (1992).
[58]H. J. Monkhorst and J. D. Pack, Phys. Rev. B **13**, 5188 (1976).
[59]M. Methfessel and A. T. Paxton, Phys. Rev. B **40**, 3616 (1989).
[60]G. Rubio-Bollinger, S. R. Bahn, N. Agraït, K. W. Jacobsen, and S. Vieiria, Phys. Rev. Lett. **87**, 026101 (2001).
[61]F. J. Ribeiro and M. L. Cohen, Phys. Rev. B **68**, 035423 (2003).
[62]N. V. Skorodumova, S. I. Simak, A. E. Kochetov, and B. Johansson, Phys. Rev. B **72**, 193413 (2005).
[63]N. V. Skorodumova, S. I. Simak, A. E. Kochetov, and B. Johansson, Phys. Rev. B **75**, 235440 (2007).
[64]A. Grigoriev, N. V. Skorodumova, S. I. Simak, G. Wendin, B. Johansson, and R. Ahuja, Phys. Rev. Lett. **97**, 236807 (2006).
[65]G. Henkelman, A. Arnaldsson, and H. Jónsson, Comput. Mater. Sci. **36**, 354 (2006).
[66]E. Sanville, S. D. Kenny, R. Smith, and G. Henkelman, J. Comput. Chem. **28**, 899 (2007).